

# Spontaneous formation of chaotic protrusions in a polymerizing active gel layer

N. Levernier<sup>1,2</sup> and K. Kruse<sup>1,2,3</sup>

<sup>1</sup>Department of Biochemistry, University of Geneva, Geneva, Switzerland

<sup>2</sup>Department of Theoretical Physics, University of Geneva, Geneva, Switzerland

<sup>3</sup>National Center of Competence in Research Chemical Biology, University of Geneva, Geneva, Switzerland

The actin cortex is a thin layer of actin filaments and myosin motors beneath the outer membrane of animal cells. It determines the cells' mechanical properties and forms important morphological structures. Physical descriptions of the cortex as a contractile active gel suggest that these structures can result from dynamic instabilities. However, in these analyses the cortex is described as a two-dimensional layer. Here, we show that the dynamics of the cortex is qualitatively different when gel fluxes in the direction perpendicular to the membrane are taken into account. In particular, an isotropic cortex is then stable for arbitrarily large active stresses. If lateral contractility exceeds vertical contractility, the system can either form protrusions with an apparently chaotic dynamics or a periodic static pattern of protrusions.

The cytoskeleton is a dynamic meshwork of filamentous protein assemblies that is of crucial importance for living cells [1–3]. The filaments, formed by the proteins actin or tubulin, interact with molecular motors like myosins or kinesins. By using a chemical fuel, these are able to generate mechanical stresses in the filament network turning the network into an active gel [4]. Physical studies of active matter often use a hydrodynamic approach [5]. For the cytoskeleton, this approach has been used to study structures and dynamics that are either alien to conventional matter or behave differently from their passive counterparts. Examples include topological point defects [4, 6–11], spontaneous flow transitions [12–14], or buckling instabilities of contracting gels [15, 16].

Physical tools and concepts have also been used to study structures formed by the cytoskeleton in living cells. In this context, the actin cortex – a thin actomyosin layer beneath the plasma membrane of animal cells – is of particular interest. It determines the mechanical properties of animal cells [17, 18] and plays an important role in cellular morphogenesis [19]. In addition, the cortex hosts a number of important cytoskeletal structures [20]. A particularly important example is the contractile actomyosin ring that cleaves animal cells into two daughter cells during late stages of division. The ring might be generated by a dynamic instability of the cortex [21, 22] and its dynamics when connected to a membrane have been studied [23, 24].

The cortex is formed by actin filaments that polymerize directly at the cell membrane [3]. Its thickness, which has been reported to be of a few hundred nanometers [25, 26], is determined by the actin polymerization velocity and its disassembly rate [27]. Due to the large aspect ratio, in theoretical analysis, the cortex is typically considered as a two-dimensional surface [28–31]. However, a formal reduction of the dynamics to the two lateral dimensions as in a thin-film approximation is not always possible.

In this work, we explore the dynamics of a thin layer of a contractile active gel on a rigid substrate with a con-

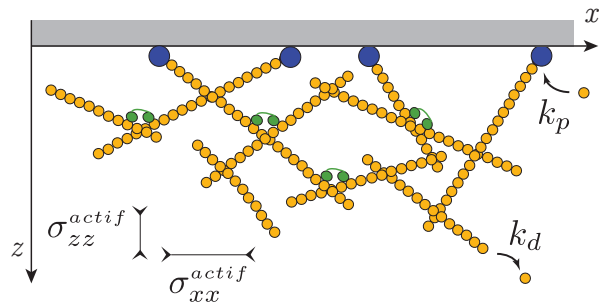


FIG. 1. Illustration of an anisotropic active gel polymerizing on a surface. Assembly of the filaments (yellow) at  $z = 0$  is mediated by nucleators (blue) of density  $\rho_0$ . This leads to a flux of gel  $k_p \delta \rho_0$  perpendicular to the surface, where  $k_p$  is the polymerization rate and  $\delta$  the length added to a filament upon addition of a subunit. The gel disassembles in the bulk at a constant rate  $k_d$ . Active stress is generated by motor proteins (green).

stant influx of material at the boundary. Contrary to previous work, we also account for gel flows in the dimension perpendicular to the substrate. We find that an isotropic layer is always stable against perturbations. In case, active contractile stresses are stronger in the lateral direction than perpendicular to the substrate, we observe an instability leading to a local increase in gel density similar to the dynamics within the thin-layer approximation [30–32]. However, the states emerging in our system differ fundamentally from those reported previously: we find periodic stationary states and states that are apparently chaotic. In both cases, they exhibit a characteristic length scale, which is not the case when treating the system in two dimensions.

We consider a three-dimensional viscous active gel, growing into the half space  $z \geq 0$  at the surface ( $x, y, z = 0$ ). For the sake of simplicity, we assume invariance along the direction  $y$ , see Fig. 1. The state of the gel is determined by its density  $\rho$  and its velocity  $\mathbf{v} = (v_x, v_z)$ .

Mass conservation and force balance yield:

$$\partial_t \rho + \partial_x(\rho v_x) + \partial_z(\rho v_z) = -k_d \rho \quad (1)$$

$$\eta [2\partial_{xx} v_x + \partial_{xz} v_x + \partial_{zz} v_z] = \partial_x \Pi_x(\rho) \quad (2)$$

$$\eta [2\partial_{zz} v_z + \partial_{xz} v_z + \partial_{xx} v_x] = \partial_z \Pi_z(\rho). \quad (3)$$

In these equations,  $k_d$  is the gel's disassembly rate,  $\eta$  denotes the viscosity and  $\Pi_{x,z}$  are the components of the non-viscous contributions to the total stress, which we assume to have only diagonal components. The non-viscous stress has two contributions: an effective hydrostatic pressure and the stress generated by active processes in the gel. In an acto-myosin gel, the latter result from the action of molecular motors and from actin-filament assembly. In general, both contributions could be anisotropic due to local filament alignment. For simplicity, we consider an isotropic hydrostatic pressure and an active stress with fixed anisotropy. Accordingly, we do not consider orientational order of the filaments to be a dynamic field. We discuss the limitations of this assumption at the end of our manuscript. Similar to Ref. [27], we choose

$$\Pi_{x,z}(\rho) = a_{x,z} \rho^3 + b \rho^4 \quad (4)$$

with  $b > 0$ . We take  $a_{x,z} < 0$  reflecting the contractile nature of the active stress. Consequently,  $\Pi_x$  and  $\Pi_z$  decrease with  $\rho$  for low enough densities and increase with  $\rho$  as  $\rho \rightarrow \infty$ . We checked that our results do not depend on the specific form chosen for  $\Pi_{x,z}$ . It suffices that the dependence of  $\Pi_{x,z}$  on  $\rho$  is non-monotonous.

The dynamic equations are completed with the boundary condition  $\rho(z=0) = \rho_0$  and  $v_z(z=0) = v_p$ , where  $\rho_0$  is the density of nucleators at the boundary and  $v_p$  the polymerization speed. In addition, the tangential stress at the surface is balanced by friction of the gel along the membrane:

$$\eta \partial_z v_x|_{z=0} = \xi v_x(z=0), \quad (5)$$

where  $\xi$  is the friction constant. Furthermore, we impose periodic boundary conditions in the  $x$ -direction with period  $L$ . In the  $z$ -direction, the system extends to infinity and  $\rho \rightarrow 0$  for  $z \rightarrow \infty$ .

If we ignore the  $z$ -direction in Eqs. (1)-(3), we arrive at a dynamic system similar to others that have been used before in the analysis of the actin cortex or other thin active gel layers [30–32]. For high enough activity, these systems typically generate contracted stationary states with a single region of high gel density.

In the following we will use a dimensionless form of the dynamic equations (1)-(4) and scale time by  $k_d^{-1}$ , length by  $\ell = v_p k_d^{-1}$ , concentration by  $\rho_0$ , and stress by  $\eta k_d$ . Hence, the relevant parameters are  $a_{x,z} k_d^{-1} \rho_0^{-3} \eta^{-1}$ ,  $b k_d^{-1} \eta^{-1} \rho_0^{-4}$ , and  $\xi k_d (v_p \eta)^{-1}$ . We will use the same notation for the original and the rescaled parameters.

For future use, we introduce the anisotropy parameter  $\epsilon = a_x/a_z$ .

In case the gel is invariant with respect to lateral translations, two qualitatively different stationary states exist: either the density decays exponentially or it jumps from a finite value  $\rho_e$  to zero at  $z = h \sim \ell$  [27]. For the "exponential profile", the velocity  $v_z$  converges to a finite value for  $z \rightarrow \infty$ . In contrast,  $v_z = 0$  for  $z > h$  for the "step profile". The latter is only possible for large enough contractility, that is, for values of  $a_z$  below a critical value  $a_c \leq 0$ . In this case, also the density of nucleators  $\rho_0$  needs to exceed a critical value  $\rho_c$ . Otherwise, the profile decays exponentially.

We start our analysis of the general case by numerically solving the dynamic equations (1)-(4). In each time step, we first determine the velocity field through the force balance equations (2) and (3), where we use Fourier decomposition along  $x$  and finite-differences along  $z$ . We then update the density, where the derivatives in  $x$ -direction are first evaluated in Fourier space. The contribution of  $\partial_z(\rho v_z)$  is obtained by an up-wind finite-differences scheme in real space. To improve the stability of the scheme, we have added a diffusion term with diffusion constant  $D = 10^{-3}$  to the mass conservation equation (1). In all simulations, we use  $\Delta x = 0.004$ ,  $\Delta z = 0.007$ , and  $\Delta t = 0.0005$ . We checked that our results do not change for smaller values. As initial condition, we take  $\rho(x_i, z_j) = \rho_0(z_j)(1 + \tilde{\eta}(x_i, z_j))$ , where  $\tilde{\eta}(x_i, z_j)$  are independent and uniformly distributed random numbers between  $-0.05$  and  $0.05$ .

We first consider the limit of zero friction, i.e.,  $\partial_z v_x(z=0) = 0$ . If  $a_z < a_c$ , then there is a critical anisotropy  $\epsilon_c$ , such that the step profile is unstable for  $\epsilon > \epsilon_c$ . In Figure 2 and Movie 1 [33], we present the solution for  $a_z = -7 < a_c$  and  $\epsilon = 1.18 > \epsilon_c$ . Locally, the gel contracts laterally, which leads to the formation of finger-like protrusions growing into the direction of increasing  $z$ . Strikingly, the protrusions stay dynamic: neighboring protrusions merge and new ones appear continuously, such that the system never reaches a steady state. As can be seen in the kymograph, Fig. 2, the system does not settle in a periodic state either. Instead the dynamics appears to be chaotic. Our numerical results indicate that the chaotic state presented in Fig. 2 emerges directly at the critical anisotropy  $\epsilon_c$ . Such a direct transition to chaotic dynamics, which is impossible for systems with a finite number of degrees of freedom, is known to exist for other spatially extended dynamic systems [34, 35].

Note that for  $\xi = 0$ ,  $\ell$  is the only length scale present in our system, such that it also fixes the order of the density of protrusions in addition to the thickness of the step profile. When reducing the lateral extension  $L$  sufficiently, the system forms a single protrusion for  $\epsilon > \epsilon_c$ , which is now stationary. In that case, new material that is introduced into the system at  $z = 0$  is drawn into the protrusion by the contractile lateral activity and cannot

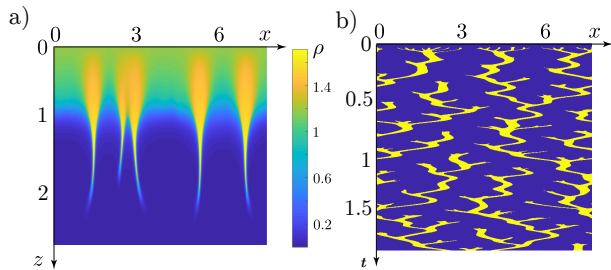


FIG. 2. Chaotic state of continuously appearing and merging protrusions in the case of low friction. a) Snapshot of the density field  $\rho$ . b) Kymograph of the density at  $z = h$  with values  $\rho > \rho_e$  shown in yellow. Parameters are  $L = 8.2$ ,  $\epsilon = 1.25$ ,  $a_z = -7$ ,  $b = 4.9$ ,  $\xi k_d / (v_p \eta) = 0$  and  $\rho_0 = \rho_e = 1.18$ .

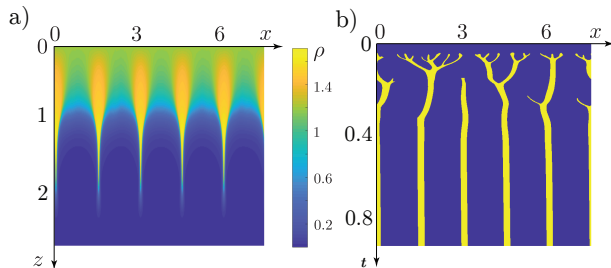


FIG. 3. Stationary periodic pattern in the case of high friction. a) Snapshot of the density field  $\rho$ . b) Kymograph of the density at  $z = h$  with values  $\rho > \rho_e$  shown in yellow. Parameters are  $L = 8.2$ ,  $\epsilon = 1.25$ ,  $a_z = -7$ ,  $b = 4.9$ ,  $\xi k_d / (v_p \eta) = 5$  and  $\rho_0 = \rho_e = 1.18$ .

form a new protrusion. In the case of large enough friction  $\xi$ , a stationary state emerges at the instability. It consists of a periodic arrangement of protrusions, Fig. 3 and Movie 2 [33]. Increasing the activity further, this state loses stability in favor of the chaotic dynamics described above.

To better understand the mechanism underlying the instability of the states homogenous in  $x$ , we first perform a linear stability analysis of the step profile with  $\rho_0 = \rho_e$ . Then  $\rho(x, z) = \rho_0$  for  $0 \leq z \leq h$  and zero otherwise. Note that this state only exists if  $a_z \leq a_c$ . Let  $\alpha = \frac{d\Pi_x}{d\rho}|_{\rho_e}$  and  $\beta = \frac{d\Pi_z}{d\rho}|_{\rho_e}$ . Then, the growth rate  $s$  of a perturbation  $\tilde{\rho} \exp(iq_x x + iq_z z)$  for  $0 \leq z \leq h$  is given by

$$s = -\frac{\rho_e}{2} \left( \beta + (\alpha - \beta) \frac{q_x^2}{q_x^2 + q_z^2} \right) \quad (6)$$

with real wave numbers  $q_x$  and  $q_z$ . Hence, the step profile is unstable if  $\alpha$  is negative. In this case, a local increase of the gel density leads to a local increase of the contractility in  $x$ -direction. In turn, this generates flows toward the region of increased density, leading to a further increase. The most unstable modes  $\mathbf{q} = (q_x, q_z)$  are  $(q_x, 0)$  for any  $q_x$  and  $(\infty, q_z)$  for any finite  $q_z$ . Consequently, the linear stability analysis does not suggest an intrinsic

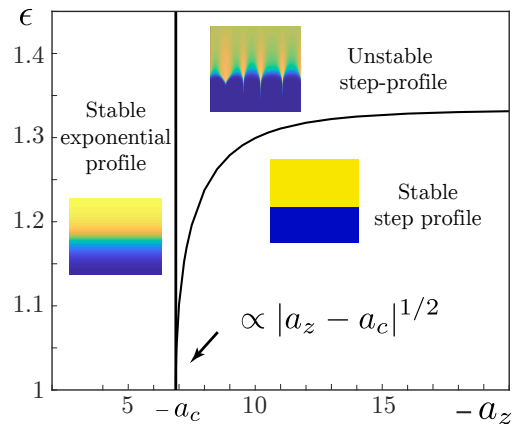


FIG. 4. Stability diagram. For  $0 > a_z > a_c$  with  $a_c$  denoting the critical activity for the transition from an exponential decaying density to one jumping to zero at  $z = h$  [27], the steady state is linearly stable. For  $a_z < a_c < 0$  the steady state is linearly stable as long as the anisotropy  $\epsilon$  is below a critical value. Parameters are  $b = 4.9$  and  $\rho_0 = \rho_e$  for  $a_z < a_c$ . For  $a_z > a_c$ , the system evolves into an exponential profile independently of the value of  $\rho_0$ . The value of the friction  $\xi k_d / (v_p \eta)$  is irrelevant for the stability.

characteristic wave length of the pattern beyond the instability. Since an infinite number of modes becomes simultaneously unstable, the steady state can lose stability directly in favor of a chaotic state as our numeric solution suggests for the parameter values corresponding to Fig. 2. We emphasize that for the step profile, we necessarily have  $\beta > 0$  [27]. The instability reported above requires  $\alpha < 0$  and thus  $a_x < a_z$ , i.e., an anisotropic active stress that is more contractile in the  $x$ -direction.

In Figure 4, we present the stability diagram in the plane of the activity parameter  $a_z$  and the anisotropy  $\epsilon$ . Even though the precise form of the stability boundary  $\epsilon_c(a_z)$  depends on the detailed expression of the functions  $\Pi_{x,z}$ , we always have  $\epsilon_c - 1 \propto \sqrt{a_z - a_c}$  for  $a_z \gtrsim a_c$ . Indeed,  $\frac{d\Pi_x}{d\rho}|_{\rho_e^c} = 0$ , where  $\rho_e^c \equiv \rho_e$  for  $a_z = a_c$ , so that for  $a_z = a_c + \delta a$  we get  $\rho_e - \rho_e^c \propto \sqrt{\delta a}$ . Furthermore,  $\epsilon_c$  saturates for  $a_x \rightarrow \infty$  independently of the precise form of  $\Pi_{x,z}$ . In the case the expressions for  $\Pi_{x,z}$  are given by Eq. (4), we find  $\epsilon = -4b\rho_e/a_z = O(1)$  for  $a_x \rightarrow \infty$ .

The exponential profiles are unconditionally stable. The crucial difference compared to the step profiles is that, here, the steady-state velocity  $v_z(z)$  reaches a non-zero velocity  $v_\infty$  when  $z \rightarrow \infty$ . Hence, any perturbation  $\delta\rho$  will be transported at a finite velocity away from the substrate at  $z = 0$ . As the gel degrades with time at rate  $k_d$ , the perturbation will reach a region where the density  $\rho$  is exponentially small in finite time. The perturbation then satisfies the advection-degradation equation  $\partial_t \delta\rho + v_\infty \partial_z \delta\rho = -k_d \delta\rho$ , which implies that it eventually disappears.

The linear stability analysis does not yield informa-

tion about whether the emergent state is stationary or not. The stability of the periodic stationary pattern versus the chaotic state is determined by the competition of two transport processes close to the surface. One results from the polymerization of new material at the surface, which occurs at velocity  $v_p$ , whereas the other results from the attraction of neighboring protrusions, which approach each other at a typical velocity  $v_{\text{approach}} \equiv v_p \eta (\xi \ell)^{-1}$ . Consider a nascent protrusion at  $z \sim \ell$ . For  $v_p \lesssim v_{\text{approach}}$ , it will be sucked up by an existing neighboring protrusion before it can mature and reach a length similar to  $\ell$ . In the opposite case, it is advected away from the substrate at  $z = 0$  before it fuses with a neighboring protrusion. In the first case, the stationary period pattern is stable, in the second the apparently chaotic state emerges. The transition between the chaotic and the periodic pattern occurs when both velocities are of the same order, that is, for  $\eta/\xi \sim \ell$ . Indeed,  $0 = v_{\text{approach}} < v_p$  in Fig. 2, whereas  $5 = v_{\text{approach}} > v_p$  in Fig. 3.

In this letter, we have shown that the dynamics of an active gel polymerizing at a surface is fundamentally different from the dynamics of this system, when fluxes perpendicular to the surface are neglected. In fact, there is no way to integrate the dynamic equations (1)-(3) over  $z$  to get a closed system for the averaged fields  $\bar{\rho}(x)$  and  $\bar{v}(x)$  in one dimension. Hence, results obtained within the thin-layer approximation have to be taken with caution.

Let us comment on our assumption of fixed anisotropy of the active gel. In the cytoskeleton, the differences in the active stress in the direction lateral and perpendicular to the surface result from the alignment of the filaments along the membrane. In a full description of the cytoskeleton, the filament alignment is a dynamic field and the anisotropy should emerge spontaneously. Filament alignment in the direction perpendicular to the direction of contraction is a natural feature of the dynamics of active polar or nematic gels [22]. In addition, the presence of a surface should also lead to a preferential alignment of the filaments along the boundary. We do thus not expect the dynamics to change qualitatively in presence of a dynamic orientational order field and postpone its analysis to future work.

Compared to previous analyses of thin layers of active gels, we found the existence of a characteristic length scale, a direct transition to a chaotic state, and a transition controlled by friction. Periodic patterns also emerge in multi-component active systems [32, 36–39]. In our system, a single component suffices, because contractility in combination with filament turnover can spontaneously generate a defined gel thickness, which then can lead to a periodic pattern in the  $x$ -direction. Spatiotemporal chaos in absence of inertial effects has been reported in active systems [6, 40–43]. However, these system were incompressible, did not exhibit turnover, and displayed dynamic nematic or polar order. In the two-component

system studied in Ref. [43], a transition between a static periodic and a chaotic state was obtained by changing the friction of the gel with a substrate. However, in that case the friction permeated the whole system, whereas in our case, it is restricted to a boundary. Together, these features show that adding a dimension can have similar effects to the introduction of additional physical properties.

In addition to the activity and the friction, we can also use  $\rho_0$  as a control parameter. In a living cellular, this parameter is set by the density of active actin-filament nucleators. In this way the cell has a readily accessible controller to switch between different morphologies. In upcoming work, we will analyse the dynamics of the actin cortex in case the surface is deformable as is the plasma membrane of an animal cell.

- 
- [1] D. Bray, *Cell Movements*, 2nd ed., From Molecules to Motility (Taylor & Francis, 2001).
  - [2] J. Howard, *Mechanics of Motor Proteins and the Cytoskeleton* (Sinauer Associates, Sunderland, 2001).
  - [3] B. Alberts, A. Johnson, J. Lewis, M. Raff, K. Roberts, and P. Walter, *Molecular Biology of The Cell*, 5th ed., edited by B. Alberts (Garland Science, 2008).
  - [4] K. Kruse, J.-F. Joanny, F. Jülicher, J. Prost, and K. Sekimoto, *Phys. Rev. Lett.* **92**, 078101 (2004).
  - [5] M. C. Marchetti, J. F. Joanny, S. Ramaswamy, T. B. Liverpool, J. Prost, M. Rao, and R. A. Simha, *Rev. Mod. Phys.* **85**, 1143 (2013).
  - [6] T. Sanchez, D. T. N. Chen, S. J. DeCamp, M. Heymann, and Z. Dogic, *Nature* **491**, 431 (2012).
  - [7] L. Giomi, M. J. Bowick, X. Ma, and M. C. Marchetti, *Phys. Rev. Lett.* **110**, 228101 (2013).
  - [8] S. P. Thampi, R. Golestanian, and J. M. Yeomans, *Phys. Rev. Lett.* **111**, 118101 (2013).
  - [9] L. M. Pismen, *Phys. Rev. E* **88**, 050502 (2013).
  - [10] F. C. Keber, E. Loiseau, T. Sanchez, S. J. DeCamp, L. Giomi, M. J. Bowick, M. C. Marchetti, Z. Dogic, and A. R. Bausch, *Science* **345**, 1135 (2014).
  - [11] D. J. G. Pearce, P. W. Ellis, A. Fernandez-Nieves, and L. Giomi, *arXiv* (2018), 1805.01455v1.
  - [12] R. Voituriez, J. F. Joanny, and J. Prost, *EPL (Europhysics Letters)* **70**, 404 (2007).
  - [13] S. Fürthauer, M. Neef, S. W. Grill, K. Kruse, and F. Jülicher, *New J. Phys.* **14**, 023001 (2012).
  - [14] G. Duclos, C. Blanch-Mercader, V. Yashunsky, G. Salbreux, J. F. Joanny, J. Prost, and P. Silberzan, *Nat. Phys.* **14**, 728 (2018).
  - [15] E. Hannezo, J. Prost, and J.-F. Joanny, *Proc. Natl. Acad. Sci. USA* **111**, 27 (2014).
  - [16] Y. Ideses, V. Erukhimovitch, R. Brand, D. Jourdain, J. S. Hernandez, U. R. Gabinet, S. A. Safran, K. Kruse, and A. Bernheim-Groswasser, *Nat. Comms.* **9**, 2461 (2018).
  - [17] M. Fritzsche, C. Erlenkämper, E. Moeendarbary, G. Charras, and K. Kruse, *Sci. Adv.* **2**, e1501337 (2016).
  - [18] P. Chugh, A. G. Clark, M. B. Smith, D. A. D. Cassani, K. Dierkes, A. Ragab, P. P. Roux, G. Charras, G. Salbreux, and E. K. Paluch, *Nat. Cell Biol.* **19**, 689 (2017).

- [19] G. Salbreux, G. Charras, and E. Paluch, *Trends Cell Biol.* **22**, 536 (2012).
- [20] L. Blanchoin, R. Boujemaa-Paterski, C. Sykes, and J. Plastino, *Physiol. Rev.* **94**, 235 (2014).
- [21] A. Zumdieck, M. Cosentino Lagomarsino, C. Tanase, K. Kruse, B. Mulder, M. Dogterom, and F. Jülicher, *Phys. Rev. Lett.* **95**, 258103 (2005).
- [22] G. Salbreux, J. Prost, and J. F. Joanny, *Phys. Rev. Lett.* **103**, 058102 (2009).
- [23] J. Sedzinski, M. Biro, A. Oswald, J.-Y. Tinevez, G. Salbreux, and E. Paluch, *Nature* **476**, 462 (2011).
- [24] H. Turlier, B. Audoly, J. Prost, and J.-F. Joanny, *Biophys. J.* **106**, 114 (2014).
- [25] A. G. Clark, K. Dierkes, and E. K. Paluch, *Biophys J* **105**, 570 (2013).
- [26] M. P. Clausen, H. Colin-York, F. Schneider, C. Eggeling, and M. Fritzsche, *J. Phys. D* **50**, 064002 (2017).
- [27] J. F. Joanny, K. Kruse, J. Prost, and S. Ramaswamy, *Eur. Phys. J. E* **36**, 52 (2013).
- [28] M. Mayer, M. Depken, J. S. Bois, F. Jülicher, and S. W. Grill, *Nature* **467**, 617 (2010).
- [29] S. R. Naganathan, S. Fürthauer, M. Nishikawa, F. Jülicher, and S. W. Grill, *Elife* **3**, e04165 (2014).
- [30] H. Berthoumieux, J.-L. Maitre, C.-P. Heisenberg, E. K. Paluch, F. Juelicher, and G. Salbreux, *New J. Phys.* **16**, 065005 (2014).
- [31] A. Mietke, F. Jülicher, and I. F. Sbalzarini, *Proc. Natl. Acad. Sci. USA* **116**, 29 (2019).
- [32] J. S. Bois, F. Jülicher, and S. W. Grill, *Phys. Rev. Lett.* **106**, 028103 (2011).
- [33] See Supplemental Material at [URL will be inserted by publisher] for movies of the numerical solutions.
- [34] I. S. Aranson and L. Kramer, *Rev. Mod. Phys.* **74**, 99 (2002).
- [35] M. I. Tribelsky and K. Tsuboi, *Phys. Rev. Lett.* **76**, 1631 (1996).
- [36] K. Kruse and F. Jülicher, *Phys. Rev. E* **67**, 051913 (2003).
- [37] K. Gowrishankar, S. Ghosh, S. Saha, R. C. S. Mayor, and M. Rao, *Cell* **149**, 1353 (2012).
- [38] K. V. Kumar, J. S. Bois, F. Juelicher, and S. W. Grill, *Phys. Rev. Lett.* **112**, 208101 (2014).
- [39] D. S. Banerjee, A. Munjal, T. Lecuit, and M. Rao, *Nat. Comms.* **8**, 1121 (2017).
- [40] C. Dombrowski, L. Cisneros, S. Chatkaew, R. E. Goldstein, and J. O. Kessler, *Phys. Rev. Lett.* **93**, 098103 (2004).
- [41] M. Neef and K. Kruse, *Phys. Rev. E* **90**, 052703 (2014).
- [42] R. Ramaswamy and F. Jülicher, *Sci. Rep.* **6**, 20838 (2016).
- [43] A. Doostmohammadi, M. F. Adamer, S. P. Thampi, and J. M. Yeomans, *Nat. Comms.* **7**, 10557 (2016).